From the Istituto di Mineralogia e Petrografia, Università di Trieste, Italy, and the Istituto di Mineralogia e Petrologia, Università di Padova, Italy

Crystal Structure Refinement of 13 Olivines in the Forsterite-Fayalite Series from Volcanic Rocks and Ultramafic Nodules

F. Princivalle and **L. Secco**

With 5 Figures

Summary

The results of the present paper confirm the overall dependence of the geometric parameters of olivines on the Mg/(Fe+Mn) ratio. M1 and M2 volumes linearly decrease with increasing forsterite (*Fo*) content but at different rates. The difference between the volumes of the octahedral sites decreases gradually from *Fo* 92% to *Fo* 50% and then remains virtually constant down to *Fo* 0.2%.

Fe(M1)/Fe(M2) ratios indicate that Fe^{2+} prefers the M1 site in fayalite (*Fa*)-rich olivines (*Fa* = 39% to 92%; average Fe(M1)/Fe(M2) = 1.04 ± 0.02). Instead, in Mg-olivines (*Fo* = 80% to 92%) a Mg-M1 preference (average Mg(M1)/Mg(M2) = 0.96 ± 0.05) may exist. Finally, Mn(M1)/Mn(M2) ratios do not indicate a definite Mn preference for M2 in the studied olivines (MnO = 0.44% to 4.5 wt.%; average Mn(M1)/Mn(M2) = 0.99 ± 0.13).

No relevant influence on geometric parameters was observed between Ca-free and Ca-bearing (maximum CaO = 0.66 wt.%) olivines.

Zusammenfassung

Struktur-Verfeinerung von 13 Olivinen der Forsterit-Fayalit-Serie aus Vulkaniten und ultramafischen Einschlüssen

Die Ergebnisse dieser Untersuchung bestätigen die Abhängigkeit der geometrischen Parameter der Olivine vom Verhältnis Mg/(Fe+Mn). Die Volumina M1 und M2 nehmen linear, jedoch jeweils verschieden, mit zunehmenden Forsterit (*Fo*)-Gehalt ab. Der Unterschied zwischen den Volumina der oktaedrischen Plätze nimmt graduell von *Fo* 92% bis *Fo* 50% ab und bleibt dann bis zu *Fo* 0,2% konstant.

Fe(M1)/Fe(M2)-Verhältnisse zeigen, daß Fe^{2+} vorzugsweise M1 Plätze in fayalitreichen Olivinen (*Fa* = 39% bis 92%; durchschnittliches Fe(M1)/Fe(M2) = 1,04 ± 0,02) besetzen. In Mg-Olivinen (*Fo* = 80% bis 92%) hingegen dürfte eine Mg-M1 Präferenz vorliegen (durchschnittliches Mg(M1)/Mg(M2) = 0,96 ± 0,05). Mn(M1)/Mn(M2)-Verhältnisse weisen nicht auf eine definitive Mn-Präferenz für M2 in den untersuchten Olivinen hin (MnO = 0,44–4,5 wt.%; durchschnittliches Mn(M1)/Mn(M2)-Verhältnis = 0,99 ± 0,13).

Der Calcium-Gehalt (Maximum, CaO = 0,66 wt.%) beeinflußt die geometrischen Parameter der Olivine nicht.

8*

Introduction

Mg/Fe and Mg/Mn substitution in natural and synthetic olivines has been investi-
gated by several authors (*Brown*, 1980; *Brown* and *Prewitt*, 1973; *Wenk* and
Raymond, 1973; *Basso* et al., 1979; *Francis* and *Ribbe*, 1980; *Lumpkin* and
Ribbe, 1983).

Correct determination of cation ordering in M1 and M2 octahedral sites
remains a major problem, in view of possibility of obtaining information of
petrological and petrogenetic interest.

This paper presents the results of crystal structure refinements of low-
pressure (*Fo* 81.5% to *Fo* 0.2%) and high-pressure (*Fo* 91.7% to *Fo* 89.6%)
olivines and discussing Mg, Fe^{2+} and Mn distributions between M1 and M2 sites.

Petrologic Outlines of Host Rocks

The olivines studied here occur in volcanic rocks of the Boseti Complex (Main
Ethiopian Rift; *Brotzu* et al., 1980) and in high-pressure ultramafic nodules from
the Newer Volcanics of Mt. Leura (Victoria, Australia; *Dal Negro* et al., 1984).

The Boseti volcanics are represented by (1) transitional alkaline basalts
(BO 153, 321) and strongly porphyritic basalts (BO 335); (2) trachyte (BO 421:
normative quartz (*Q*) = 4.49% and mol. $(Na_2O + K_2O)/Al_2O_3$ (A.I.) = 0.96);
(3) alkali rhyolites (BO 157, 174: *Q* = 19.91% and 18.33% respectively, A.I. =
0.99); (4) comenditic trachyte (BO 397: *Q* = 7.03%, A.I. = 1.21); (5) comendite
(BO 154: *Q* = 21.03%, A.I. = 1.05) and (6) trachytic pantellerite (BO 168:
Q = 13.31, A.I. = 1.24).

The pheno- and/or microphenocryst assemblages of the basic rocks are made
up of olivine, plagioclase, Ca-rich pyroxene and very scarce opaques, while those
of the acidic rocks are given by olivine, plagioclase, Ca-rich pyroxene, opaques,
alkali feldspar and sometimes rare orthopyroxene.

Detailed geo-volcanological and petrogenetic studies show that the Boseti
volcanics are related to crystal fractionation processes which developed under
low-pressure (a few kilobars) and low-fO_2 (about quartz-magnetite-fayalite
buffer) conditions (*Brotzu* et al., 1980; *Ganeo*, 1982).

The Victorian nodules have modal compositions (*Dal Negro* et al., 1984)
ranging from olivine-websterite approaching the lherzolite field (LE 20) to
lherzolites (LE 8, 9, 11). Notably, LE 9 has a low orthopyroxene content (9.5%
in volume) and is therefore displaced towards the wehrlite field. The nodules
have spinel as accessory phase, and different ratios between olivine and clino-
pyroxene modal contents: LE 8 = 7.6, LE 11 = 5.3, LE 9 = 4.5, LE 20 = 1.3.

The Victorian lherzolite inclusions have been considered as residual mantle
assemblages after partial fusion and magma extraction, later modified by and
equilibrated with a fractionated mantle melt under high-pressure (spinel stability)
conditions (*Frey* and *Green*, 1974). This interpretation appears consistent with
the crystal chemistry and evolution of the clinopyroxene (*Dal Negro* et al., 1984).

Table 1. *Crystallographic Data*

Sample	LE 8	LE 11	LE 9	LE 20	BO 153	BO 321	BO 335
a (Å)	4.7624(4)	4.7619(6)	4.7625(6)	4.7635(5)	4.7688(5)	4.7704(9)	4.7861(5)
b (Å)	10.2242(5)	10.2292(6)	10.2264(7)	10.2314(6)	10.2642(6)	10.2659(8)	10.3273(6)
c (Å)	5.9908(5)	5.9919(6)	5.9912(7)	5.9947(6)	6.0071(6)	6.0130(4)	6.0307(6)
V (Å^3)	291.70	291.87	291.79	292.16	294.03	294.47	298.08
No. obs. refl.	418	401	415	395	441	543	456
R [a]	0.022	0.023	0.023	0.027	0.017	0.021	0.015
M1 el.	11.20	11.29	11.25	11.51	12.46	12.62	15.66
M2 el.	11.06	11.15	11.08	11.39	12.56	12.63	15.35

Sample	BO 421	BO 157	BO 174	BO 168	BO 397	BO 154
a (Å)	4.7901(8)	4.8207(10)	4.8256(5)	4.8269(7)	4.8245(5)	4.8267(4)
b (Å)	10.3475(8)	10.4712(8)	10.4959(6)	10.5095(8)	10.5084(7)	10.5084(6)
c (Å)	6.0423(6)	6.0933(13)	6.0960(6)	6.0980(14)	6.0996(6)	6.1028(6)
V (Å^3)	299.49	307.58	308.76	309.24	309.24	309.54
No. obs. refl.	456	433	446	445	453	448
R [a]	0.022	0.025	0.022	0.026	0.023	0.023
M1 el.	16.79	21.87	23.17	23.12	23.29	23.62
M2 el.	16.31	21.27	22.80	22.98	23.24	23.31

[a] $R = \Sigma||Fo| - |Fc||/\Sigma|Fo|$

Estimated standard errors in parentheses refer to the last digit.

Crystallographic Procedures

Small crystals ($\simeq$ 0.5 mm), directly selected from relatively thick sections, were used for data collection.

Intensity data were collected using a computer-controlled SIEMENS AED four-circle diffractometer with MoK_α radiation monochromatized by a flat graphite crystal. X-ray data collection was carried out following the same procedure for all samples listed in Table 1.

The intensities of reflections with $2° \leqslant$ theta $\leqslant 30°$ were collected using the omega-scan method; the equivalent *hkl* and *h̄kl* pairs were scanned. Three standard reflections, monitored at one-hour intervals, showed no intensity variations greater than 2%.

Intensities were corrected for absorption following the semi-empirical method of *North* et al. (1968) and the values of equivalent pairs were averaged.

All refinements were carried out in the conventional but non-standard space group *Pbnm*, without chemical constraints. Ionized atomic scattering factors (*International tables for X-ray crystallography*, 1974 and *Tokonami*, 1965) were used, and all structural sites were considered fully occupied. The best fit for the experimental data was obtained by assuming 2.5 positive charges for Si, 1.5 negative charges for 0, and complete ionization for the other cations; the choice of the scattering factors was: Mg^{2+} and Fe^{2+} for M1 and M2 sites, $Si^{2.5+}$ for T site and $O^{1.5-}$ for the three oxygens.

In the first stage of refinements, isotropic temperature factors were used. The final cycles were performed allowing all parameters (atomic coordinates, anisotropic temperature factors, M1 and M2 site occupancies, scale factor and secondary extinction coefficient) to vary until the shifts were less than the least-squares difference of the corresponding parameters. Structure factors with $F_{obs} > 3 \sigma (F_{obs})$ were considered; all observations were weighted according to unit weight. The end values of discrepancy factor R varied from 1.5% to 2.8%. All calculations were carried out using the STRUCSY program package (copyright STOE).

Chemical analyses of the same single crystal used for crystal refinements were obtained from polished sections by means of an SIEMENS ETEC-AUTOSCAN microscope operated at 15 kV. X-ray data collection was made using an EDS spectrometer (ORTEC EG and G) and quantitative analyses calculated by MAGIC program (ORTEC version), and are considered accurate to within 2–3% for all elements (see Table 2).

Crystal Chemistry

a) *Cell Parameters*

In agreement with the results of *Wenk* and *Raymond* (1973), cell parameters increase with good linearity over the investigated compositional range (a + 1.3%, b + 2.7%, c + 1.8%, V + 5.8%) (Table 1). The increases of Fe (and Mn) mainly affect parameter b. The fractional coordinates of 01 remain almost constant, while $\times(02)$ and $\times(03)$ undergo the greatest change, about 0.010.

b) *M1, M2 and T Sites*

Table 3 shows bond distances, volumes and distortion parameters for M1, M2 and T sites. Figs. 1 and 2 shows lengthening of mean $\overline{M1\text{-}O}$ and $\overline{M2\text{-}O}$ bond distances with decreasing forsterite content (see *Francis* and *Ribbe*, 1980).

This relevant linearity is mainly due to M1-O3 (almost parallel to b) and M2-O2 bond distances (Figs. 1 and 2).

Fig. 3 shows that M1 volume increases at a higher rate than that of M2 (about 8.5% and 6.6% respectively), with decreasing forsterite content. The difference between M2 and M1 volumes is almost constant (average 0.473 ± 0.010 Å^3, range 0.456–0.483 Å^3) for forsterite content up to 52.3%, while it is pro-gressively significantly higher from *Fo* 52% to *Fo* 92% (average 0.597 ± 0.059 Å^3, range 0.482–0.644 Å^3). These variations in volume differences, normalized to

Table 2. *Chemical Analyses and Cation Distribution in Octahedral Sites*

Sample	LE 8	LE 11	LE 9	LE 20	BO 153	BO 321	BO 335
SiO$_2$	41.20	41.11	41.26	40.89	39.79	39.74	36.45
FeO	7.71	7.94	8.37	9.57	17.27	18.42	33.76
MnO	0.08	0.07	0.02	0.01	0.02	0.04	0.44
MgO	50.76	50.28	50.37	49.18	43.57	42.91	29.43
CaO	0.00	0.00	0.00	0.00	0.12	0.08	0.29
NiO	0.33	0.78	0.58	0.64	0.12	0.08	0.20
Σ	100.08	100.18	100.60	100.29	100.89	101.27	100.57
Fo	91.7	91.0	90.9	89.6	81.5	80.4	60.1
Fa	7.9	8.1	8.5	9.8	18.1	19.4	38.7
Tph	0.1	0.1	0.0	0.0	0.0	0.0	0.6
Lar	0.0	0.0	0.0	0.0	0.2	0.1	0.4
NiO	0.3	0.8	0.6	0.6	0.2	0.1	0.2
M1 occ. Mg	0.914	0.907	0.907	0.893	0.821	0.803	0.593
M1 occ. Fe	0.079	0.077	0.082	0.095	0.176	0.195	0.397
M1 occ. Mn	0.001	0.001	0.000	0.000	0.000	0.000	0.006
M1 occ. Ni	0.006	0.015	0.011	0.012	0.003	0.002	0.004
M2 occ. Mg	0.921	0.914	0.912	0.899	0.810	0.805	0.610
M2 occ. Fe	0.078	0.085	0.088	0.101	0.187	0.192	0.377
M2 occ. Mn	0.001	0.001	0.000	0.000	0.000	0.001	0.005
M2 occ. Ca	0.000	0.000	0.000	0.000	0.003	0.002	0.008
FeM1/FeM2	1.01	0.91	0.93	0.94	0.94	1.02	1.05

Sample	BO 421	BO 157	BO 174	BO 168	BO 397	BO 154
SiO$_2$	35.60	31.58	30.61	30.88	30.78	29.83
FeO	38.48	58.84	63.98	66.56	66.27	65.68
MnO	1.44	3.94	4.07	4.49	4.40	4.72
MgO	24.95	6.94	2.49	1.19	1.15	0.08
CaO	0.20	0.29	0.54	0.51	0.66	0.61
NiO	0.15	0.00	0.00	0.00	0.00	0.00
Σ	101.18	101.59	101.69	103.63	103.26	100.92
Fo	52.3	16.3	6.1	2.9	2.8	0.2
Fa	45.6	77.9	87.3	90.1	90.0	92.0
Tph	1.7	5.3	5.6	6.1	6.1	6.7
Lar	0.3	0.5	1.0	0.9	1.1	1.1
NiO	0.1	0.0	0.0	0.0	0.0	0.0
M1 occ. Mg	0.507	0.149	0.056	0.028	0.028	0.001
M1 occ. Fe	0.474	0.798	0.889	0.913	0.908	0.938
M1 occ. Mn	0.016	0.053	0.055	0.059	0.064	0.061
M1 occ. Ni	0.003	0.000	0.000	0.000	0.000	0.000
M2 occ. Mg	0.537	0.178	0.065	0.029	0.028	0.003
M2 occ. Fe	0.438	0.760	0.858	0.889	0.892	0.902
M2 occ. Mn	0.018	0.052	0.058	0.064	0.057	0.073
M2 occ. Ca	0.007	0.010	0.019	0.018	0.023	0.022
FeM1/FeM2	1.08	1.05	1.04	1.03	1.02	1.04

The sum of M1, M2 and T sites occupancies, calculated on the basis of four oxygens, is respectively equal to 1.000.

Table 3. *Polyhedral Geometry*

Sample	LE 8	LE 11	LE 9	LE 20	BO 153	BO 321	BO 335
Si-O1	1.615(2)	1.615(2)	1.615(2)	1.614(3)	1.616(2)	1.617(2)	1.618(2)
Si-O2	1.655(2)	1.655(2)	1.655(2)	1.659(3)	1.653(2)	1.653(2)	1.654(1)
2xSi-O3	1.635(2)	1.637(2)	1.635(2)	1.635(2)	1.636(1)	1.636(1)	1.637(1)
Average	1.635	1.636	1.635	1.636	1.635	1.636	1.636
Si-Si	3.631(1)	3.631(1)	3.631(1)	3.635(1)	3.644(1)	3.647(1)	3.668(1)
V(T)	2.207	2.210	2.207	2.210	2.208	2.212	2.216
σ^2 a	48.98	48.59	49.89	48.48	46.71	45.69	43.68
2xM1-O1	2.090(1)	2.089(1)	2.089(1)	2.089(2)	2.095(1)	2.096(1)	2.105(1)
2xM1-O2	2.072(1)	2.075(2)	2.073(1)	2.075(2)	2.080(1)	2.082(1)	2.093(1)
2xM1-O3	2.140(1)	2.142(1)	2.140(1)	2.141(2)	2.152(1)	2.153(1)	2.175(1)
Average	2.101	2.102	2.101	2.102	2.109	2.110	2.124
V(M1)	11.862	11.882	11.859	11.885	11.986	12.001	12.212
σ^2 b	99.02	98.86	99.33	98.04	102.79	103.15	109.03
M2-O1	2.179(2)	2.183(2)	2.181(2)	2.186(3)	2.188(2)	2.188(2)	2.199(1)
M2-O2	2.059(2)	2.056(2)	2.058(2)	2.057(3)	2.067(2)	2.067(2)	2.083(1)
2xM2-O3	2.222(2)	2.221(2)	2.219(2)	2.224(2)	2.232(2)	2.239(1)	2.253(1)
2xM2-O3'	2.066(2)	2.067(2)	2.069(2)	2.067(2)	2.067(1)	2.065(1)	2.065(1)
Average	2.136	2.136	2.136	2.138	2.142	2.144	2.153
V(M2)	12.500	12.496	12.503	12.528	12.593	12.617	12.745
σ^2 b	93.91	93.89	93.45	93.92	97.67	98.64	104.16
ΔV oct.c	5.10	4.91	5.15	5.13	4.82	4.38	4.18

Sample	BO 421	BO 157	BO 174	BO 168	BO 397	BO 154
Si-O1	1.619(3)	1.625(3)	1.623(3)	1.627(4)	1.623(3)	1.625(3)
Si-O2	1.652(3)	1.650(3)	1.651(3)	1.654(4)	1.650(3)	1.652(3)
2xSi-O3	1.637(2)	1.633(2)	1.636(2)	1.636(2)	1.633(2)	1.637(2)
Average	1.636	1.635	1.637	1.638	1.635	1.638
Si-Si	3.677(1)	3.724(1)	3.726(1)	3.731(1)	3.728(1)	3.731(1)
V(T)	2.216	2.215	2.220	2.226	2.213	2.224
σ^2 a	42.57	36.59	39.01	38.45	37.78	38.23
2xM1-O1	2.109(2)	2.125(2)	2.124(2)	2.127(2)	2.129(2)	2.126(2)
2xM1-O2	2.100(2)	2.121(2)	2.127(2)	2.123(3)	2.124(2)	2.126(2)
2xM1-O3	2.182(2)	2.224(2)	2.227(2)	2.234(2)	2.232(2)	2.232(2)
Average	2.130	2.157	2.160	2.161	2.162	2.161
V(M1)	12.299	12.679	12.725	12.747	12.748	12.749
σ^2 b	112.70	127.19	127.84	129.39	130.40	129.23
M2-O1	2.199(3)	2.236(3)	2.247(3)	2.241(4)	2.243(3)	2.247(3)
M2-O2	2.086(3)	2.115(3)	2.114(3)	2.122(4)	2.120(3)	2.119(3)
2xM2-O3	2.257(2)	2.295(2)	2.291(2)	2.294(3)	2.295(2)	2.296(2)
2xM2-O3'	2.068(2)	2.072(2)	2.078(2)	2.076(3)	2.079(2)	2.078(2)
Average	2.156	2.181	2.183	2.184	2.185	2.186
V(M2)	12.781	13.152	13.198	13.203	13.217	13.232
σ^2 b	107.03	121.80	122.46	123.94	124.88	123.93
ΔV oct.c	3.77	3.60	3.58	3.45	3.55	3.65

a) $\sigma(tet)^2 = \sum\limits_{i=1}^{6} (\theta_i - 109.47°)^2/5$;   b) $\sigma(oct)^2 = \sum\limits_{i=1}^{12} (\theta_i - 90°)^2/11$;   (Robinson *et al.*, 1971).
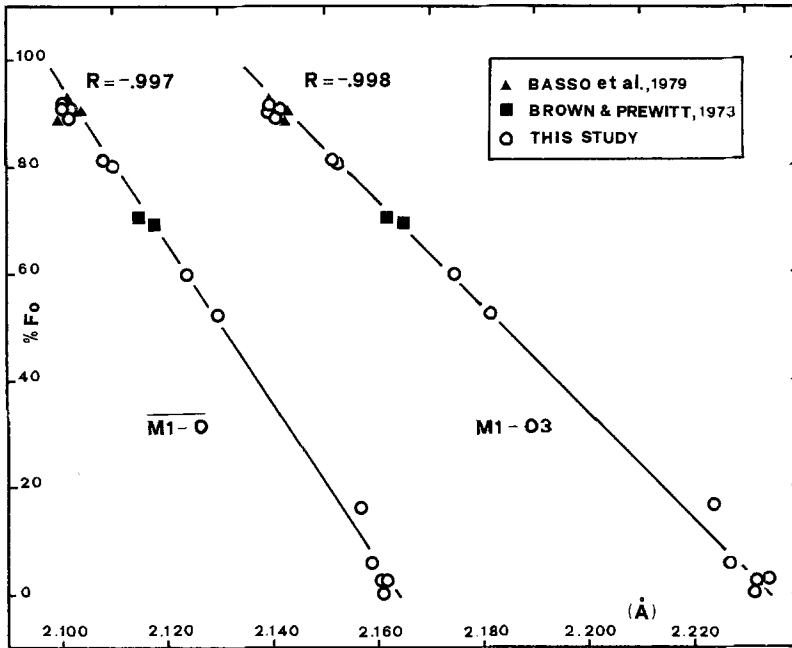
c) ΔV oct. = 100x(VM2-VM1)/VM2.

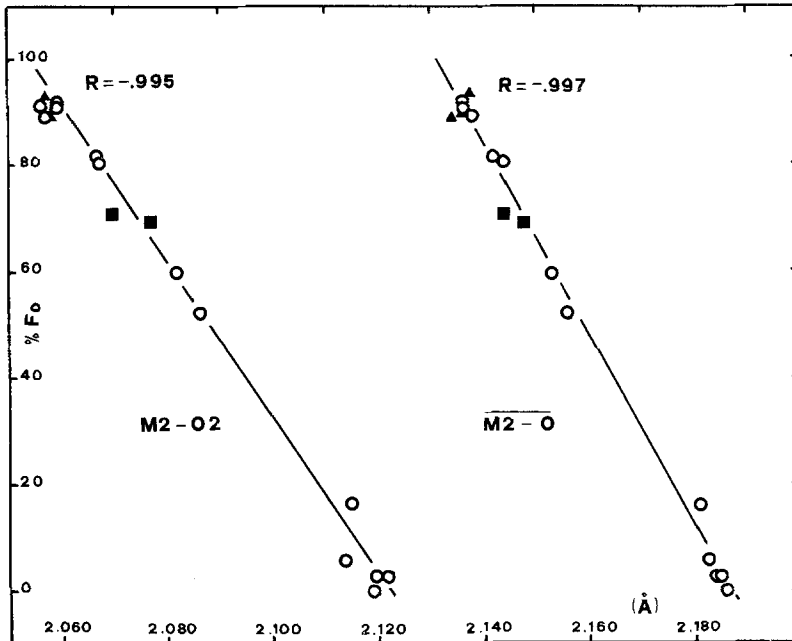Fig. 1. M1-O3 and average $\overline{M1\text{-}O}$ bond distances vs. *Fo%* content

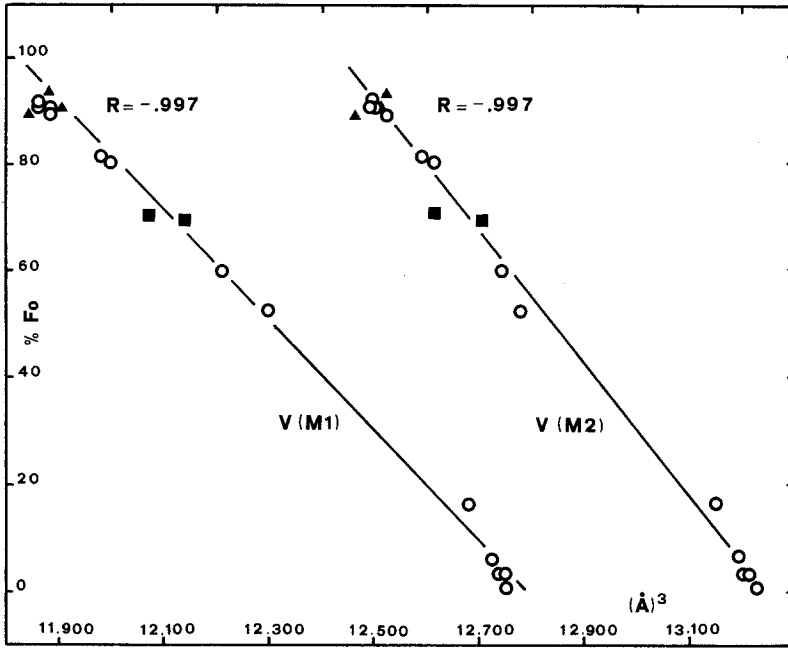Fig. 2. M2-O2 and average $\overline{M2\text{-}O}$ bond distances vs. *Fo%* content

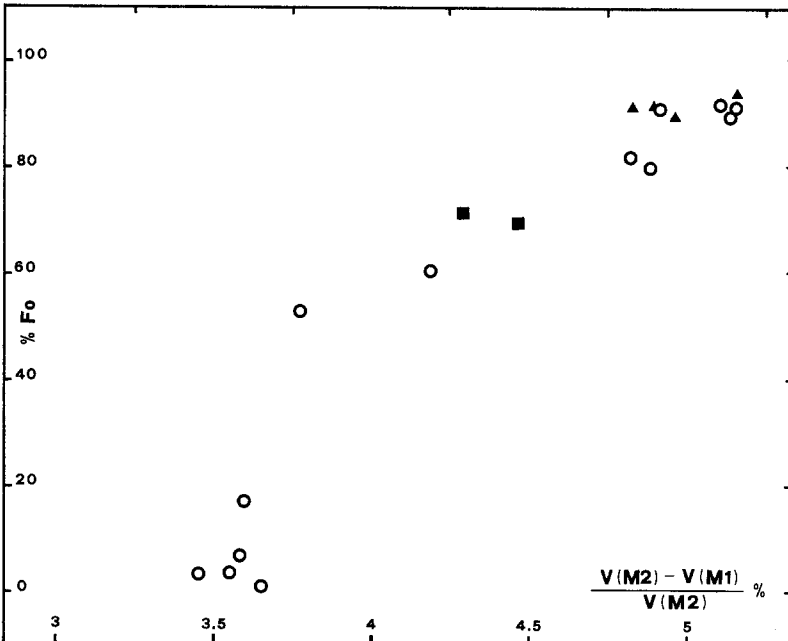Fig. 3. M1 and M2 octahedral volumes vs. *Fo%* content

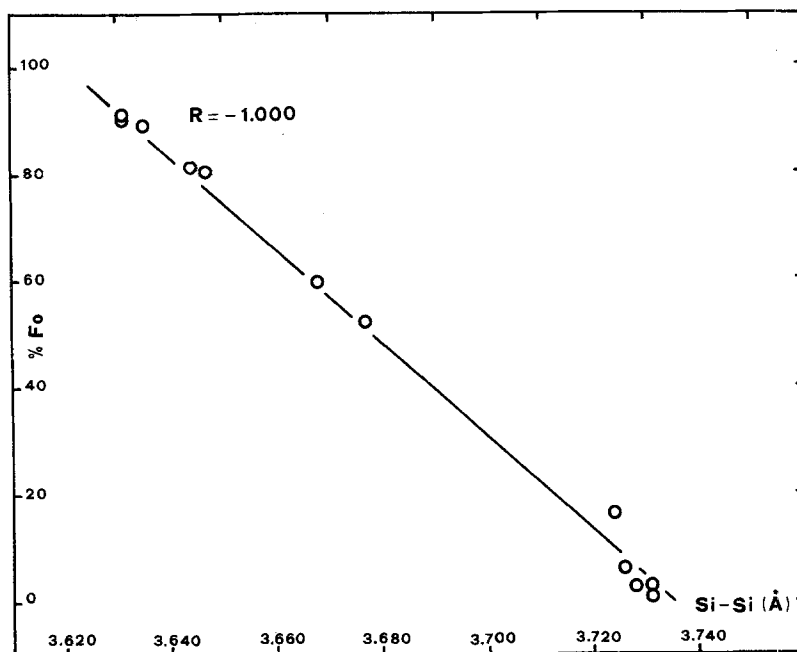Fig. 4. Percentual difference between M2 and M1 volumes vs. *Fo%* content

Fig. 5. Si-Si distance vs. *Fo%* content

M2 volume (ΔV oct.), are shown in Fig. 4. ΔV oct. regularly increases in the *Fo* 52%–92% range (3.8% to 5.1%) while for *Fo* < 50% it is about 3.6 ± 0.1%.

ΔV oct. seems to be the only parameter to which no simple linear correlation with chemical composition applies. Fig. 4 includes several data from literature which confirm this ΔV oct.-*Fo* behaviour. Clearly, ΔV oct. cumulates several very small "non-linear" effects from structural geometric parameters, but none of them is strong enough to be evidenced by a simple linear correlation analysis. Tentatively we suggest that ΔV oct. behaviour may explain the non-linearity observed by *Jambor* and *Smith* (1964) in interplanar distance *d* (174).

In this picture it is interesting that the atomic arrangement that takes place for *Fo* < 50% also leads to less compact packing; in the more fayalitic terms, interatomic voids undergo an increase of about 3% with respect to forsteritic ones. This is accompanied by a small but definite (about 0.8%) increase in tetrahedron volume. In the present study the Si-01 distance increases from 1.614(3) Å (sample LE 20, *Fo* 89.6%) to 1.627(4) Å (sample BO 168, *Fo* 2.9%), contrary to the results of *Francis* and *Ribbe* (1980).

Table 4 gives the variations of tetrahedral and octahedral distortions, calculated according to *Robinson* et al. (1971). The entrance of cations greater than Mg^{2+} causes the T site to become less distorted; its angular variance is the only geometric parameter which increases with *Fo* content.

The Si-Si distance (Fig. 5) also changes linearly with chemical composition.

Finally, it is noteworthy that high-pressure olivines show geometrical variations which fit those defined by low-pressure olivines quite well, since all the

least-squares straight lines in Fig. 1 to 5 were calculated taking only the low-pressure Boseti samples into account.

Cation Ordering in M1 and M2 Octahedra

The problems inherent in cation ordering in natural olivines in terms of valences, electronegativities and crystal field stabilization energy (CFSE) have recently been pointed out by *Lumpkin* and *Ribbe* (1983). These authors state that "CFSE causes Fe^{2+} to prefer M1, but its slightly larger size causes it to prefer M2. Crystallization and annealing conditions are important, too."

Many olivines are essentially disordered or contain more Fe^{2+} in M1 than in M2 (*Virgo* and *Hafner*, 1972; *Basso* et al., 1979), in a few olivines Fe^{2+} prefers M2 (*Wenk* and *Ramond*, 1973).

In order to obtain the best cation distribution, we used the following equations:

$$eMg \times XMg(M1) + eFe \times XFe(M1) + eMn \times XMn(M1) + eNi \times XNi = e(M1)$$
$$XMg(M1) + XFe(M1) + XMn(M1) + XNi = 1$$
$$eMg \times XMg(M2) + eFe \times XFe(M2) + eMn \times XMn(M2) + eCa \times XCa = e(M2)$$
$$XMg(M2) + XFe(M2) + XMn(M2) + XCa = 1$$
$$XMg(M1) + XMg(M2) = Mg_{tot} \text{ (microprobe)}$$
$$XFe(M1) + XFe(M2) = Fe_{tot} \text{ (microprobe)}$$
$$XMn(M1) + XMn(M2) = Mn_{tot} \text{ (microprobe)}$$

where X's represent the fraction of atoms in the site (see Table 2), e(M1) and e(M2) the number of electrons obtained from structure refinement in M1 and M2, eFe etc., the atomic number of iron, etc. (see Table 1).

Ni and Ca were completely allotted to M1 and M2 respectively on the basis of their ascertained site preference (*Nord* et al., 1982; *Brown*, 1980). All parameters (X's, e(M1), e(M2), Mg_{tot}, Fe_{tot}, Mn_{tot}) were allowed to vary simultaneously. Minimization was performed through the computer program MINUIT (*James* and *Ross*, 1975) with very satisfactory results. The sum of the square residuals of the seven equations was always less than 10^{-10}, and none of the parameters reached the limits inposed on the basis of their standard deviations.

The ratio Fe(M1)/Fe(M2) is reported in Table 2. In the examined series, Fe^{2+} slightly prefers the smaller but more distorted M1 site in iron-rich olivines. In more forsteritic terms, when M1 site becomes much smaller than M2, there is some tendency to anti-ordering.

It is noticeable that Mn shows no definite preference for M2, contrary to its behaviour in tephroitic terms.

References

Basso, R., Dal Negro, A., Della Giusta, A., Rossi, G., 1979: Fe/Mg distribution in the olivines of ultramafic nodules from Assab (Ethiopia). N. Jb. Min. Mh. *5,* 197–202.

Brotzu, P., Morbidelli, L., Piccirillo, E. M., Traversa, G., 1980: Volcanological and magmatological evidences of Boseti Volcanic Complex (Main Ethiopian Rift). In Geodynamic evolution of the Afro-Arabic Rift System. Atti dei Convegni dei Lincei. Acc. Naz. dei Lincei 4, *47,* 317–366.

Brown, G. E., 1980: Olivines and silicate spinels. In: Reviews in Mineralogy, Vol. 5, Orthosilicates (*Ribbe, P. H.,* ed.), pp. 275–381. Mineralogical Society of America, Washington, D.C.

Brown, G. E., Prewitt, C. T., 1973: High-temperature crystal chemistry of hortonolite. Amer. Min. *58,* 577–587.

Dal Negro, A., Carbonin, S., Domeneghetti, C., Molin, G. M., Cundari, A., Piccirillo, E. M., 1984: Crystal chemistry and evolution of the clinopyroxene in a suite of high-pressure ultramafic nodules from the Newer Volcanics of Victoria, Australia. Contr. Min. Petrol. (In press.)

Francis, C. A., Ribbe, P. H., 1980: The forsterite-tephroite series: I. Crystal structure refinements. Amer. Min. *65,* 1263–1269.

Frey, F. A., Green, D. H., 1974: The mineralogy, geochemistry and origin of lherzolite inclusions in Victoria basanites. Geochim. Cosmochim. Acta *38,* 1023–1059.

Ganeo, S., 1982: Studio strutturale e cristallochimico di clinopirosseni nella sequenza da basalto a pentellerite del Boseti (Rift Etiopico Principale). Unpublished graduation thesis.

International Tables for X-ray Crystallography, Vol. IV. Birmingham: Kynoch Press 1974.

Jambor, J. L., Smith, C. H., 1964: Olivine composition determination with small-diameter X-ray powder cameras. Min. Mag. *33,* 730–741.

James, F., Ross, M., 1975: A system for function minimization and analysis of the parameter errors and correlations. Computer Phys. Comm. *10,* 343–367.

Lumpkin, G. R., Ribbe, P. H., 1983: Composition, order-disorder and lattice parameters of olivines: relationships in silicate, germanate, beryllate, phosphate and borate olivines. Amer. Min. *68,* 164–176.

Nord, A. G., Annersten, H., Filippidis, A., 1982: The cation distribution in synthetic Mg-Fe-Ni olivines. Amer. Min. *67,* 1206–1211.

North, A. C. T., Phillips, D. C., Mathews, F. S., 1968: A semi-empirical method of absorption correction. Acta Cryst. *A24,* 351–359.

Robinson, K., Gibbs, G. V., Ribbe, P. H., 1971: Quadratic elongation: a quantitative measure of distortion in coordination polyhedra. Science *172,* 567–570.

Tokonami, M., 1965: Atomic scattering factor for O^{2-}. Acta Cryst. *19,* 486.

Virgo, D., Hafner, S. S., 1972: Temperature-dependent Mg, Fe distribution in a lunar olivine. Earth and Planet. Sci. Lett. *14,* 305–312.

Wenk, H. R., Raymond, K. N., 1973: Four new structure refinements of olivine. Z. Krist. *137,* 86–105.

Authors' addresses: Dr. *F. Princivalle,* Istituto di Mineralogia e Petrografia, Università di Trieste, Piazzale Europa 1, I-34127 Trieste, Italy; Dr. *L. Secco,* Istituto di Mineralogia e Petrologia, Università di Padova, Corso Garibaldi 37, I-35100 Padova, Italy.